Towards a fragility assessment of a concrete column exposed to a real fire – Tisova Fire Test

Citation for published version:
Rush, D & Lange, D 2017, 'Towards a fragility assessment of a concrete column exposed to a real fire – Tisova Fire Test', *Engineering Structures*, vol. 150, pp. 537-549.
https://doi.org/10.1016/j.engstruct.2017.07.071

Digital Object Identifier (DOI):
10.1016/j.engstruct.2017.07.071

Published In:
Engineering Structures

Towards a fragility assessment of a concrete column exposed to a real fire – Tisova Fire Test

David Rush[1]* and David Lange[2]
[1] School of Engineering,
University of Edinburgh, UK
[2] RISE Safety and Transport / Fire Research, Research Institutes of Sweden
Borås, Sweden

ABSTRACT

Fires can cause substantial damage to structures, both non-structural and structural, with economic losses of almost 1% GDP in developed countries. Whilst design codes allow engineers to design for the primary design driver, property protection is rarely, if ever, designed for. Quantification and design around property protection has been used for some time in the seismic community, particularly the PEER framework and fragility analyses. Fragility concepts have now started to be researched predominantly for steel-composite structures, however, there has been little to no research into the quantification of property protection for concrete structures, whether in design or in post-fire assessments of fire damaged structures. This paper presents selected results from the thermal environment around, and the thermal response of, a concrete column from a large scale structural fire test conducted in Tisova, Czech Republic, inside a four-storey concrete frame building, with concrete and composite deck floors. From the results of the fire test, assessments of the fire intensity are made and used to model the potential thermal profiles within the concrete column and the implications that high temperature might have on the post-fire response of the concrete column. These thermal profiles are then used to assess the reduction of the columns cross-sectional area and are compared to a quantified damage scale for concrete columns exposed to fire. This analyses presented herein will also show that common methods of defining fire intensity through equivalent fire durations do not appropriately account for the complexities of the thermal and structural response of concrete columns exposed to a travelling fire.

KEYWORDS: concrete column, travelling fire, large scale structural fire test, Tisova Fire Test, fragility assessment, damage assessment

1 INTRODUCTION

Fires can cause substantial damage to buildings, both non-structural and structural. Multiple fire-induced structural failures of buildings have been observed in recent decades (some of which are detailed in, e.g., [1]) and there is a substantial cumulative cost of fires as reflected in international fire statistics where the economic loss due to fire reaches approximately 1% of the Gross Domestic Product in developed countries [2]. Whilst current codes and design guidance (e.g. [3]) allow structural engineers to design for the principal performance driver in fire – namely life safety, comparatively little thought or guidance is typically given (with some notable exceptions) during the structural design phase of a building to the mitigation of direct and indirect losses, whether these be; economic, cultural, reputational, or environmental; that significant structural fires may cause. Furthermore, if the structural damage is known, there is relatively little information available in the literature on the repair and strengthening of fire-damaged structures [4].

Holistic, quantified 'loss' estimation for structures under extreme or accidental loads is not a novel concept, however, and there has been a recent trend towards developing probabilistic frameworks for structural fire loss estimation (e.g. [5]). This is typically undertaken in line with the Pacific Earthquake Engineering Research (PEER) framework that exists for seismic loss analysis (e.g. [6]). The seismic community have, for many years, applied concepts of '*fragility*' where the probability of a structural system reaching a given *damage state* is assessed as a function of some measure of *intensity* (e.g. peak ground acceleration used in earthquake engineering). From this assessment, designers and insurers can calculate the *expected costs* of repair or replacement of the building. Therefore, a *fragility analysis* allows designers to rationally and quantifiably account for the *risks* and *costs* associated with the *range* of possible earthquakes, and explicitly accounts for property protection as a desirable design goal.

* Corresponding author – d.rush@ed.ac.uk

When these explicit property protection goals are accounted for by the engineer in the design phase of a structure, the actual performance of the structure when the hazard occurs is vitally important to understand. For example, in 2011 an earthquake hit Christchurch, NZ, a city which was for the most part explicitly designed for seismic activity. However, the earthquake was of greater intensity than designed for and this caused a great deal of damage to the city, resulting in significant cost to repair or replace the damaged building stock and infrastructure. The high level of damage and the cost of reinstatement was shocking to the public and insurers alike, however from an engineering perspective the vast majority of buildings performed "very well" on the basis of the explicit design objectives used by the engineer to design them [7]. This public outcry also suggests that society is largely unaware of the true "performance" objectives that are used by structural engineers in design, whether for earthquake or fire engineering; it may be that a higher 'level' of property protection is actually expected by society.

Property protection is becoming more popular with building owners and insurers alike, and is now becoming frequently considered as a design driver. The level of property protection (i.e. damage level, reinstatement costs, business continuity, etc…) of structures designed for fire is generally unknown as there is no acceptable means of quantifying property protection goals (or of rationally accounting for these goals in design). Property protection is rarely explicitly considered in fire engineering design due to a lack of credible data from which to assess/model full structures in fire - this is particularly true for concrete structures [8].

Current fire engineering design methods (e.g. [9]), in general, assess structures and their response to fire on a pass/fail assessment usually consisting of prescribed fire resistance criteria and times, based almost entirely on life safety as the sole design driver. The assessment of structures to fire is usually based on a standard fire (e.g. ISO-834 [10]) that represents only one fire out of a range of possible fires which may occur, and may not represent the most onerous (or more realistic) fire insult that a structure might experience [11].

This pass / fail assessment may also be referred to as demand / capacity based design, although when analytical or numerical tools are used in structural fire engineering it is often referred to as performance based design. This is not necessarily consistent with, e.g. earthquake engineering, as discussed above, where the consequences of an event outside of failure of a structural element are considered. The difference between demand / capacity and performance based design in earthquake engineering is shown in Figure 1 (modified from [12]). Both approaches are based on an iterative approach. In demand / capacity design the iteration is based simply on a comparison of the load on the structure and the capacity of the element. If the structural elements capacity exceeds the demand placed upon it then it is deemed to satisfy the design criteria, if not then an iteration loop is performed to evaluate an element with a higher capacity. In performance based design there are two concepts added to this iteration process, consideration of the consequences of the capacity not meeting the demand (for example in financial terms or in terms of 'down-time' of the structure), and the possibility to address both the response and the consequences in a non-deterministic way. Put simply this means that although an element of structure might fail as a result of loads placed on it, bearing in mind the infrequency of the event, and so long as the actual consequences are acceptable if they happen at this frequency, then the overall design may still be acceptable.

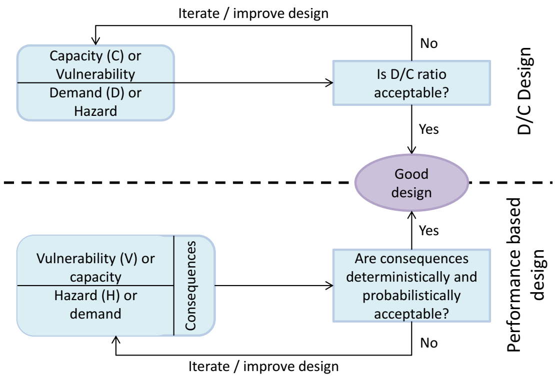

Figure 1: Demand capacity versus performance based design

Standard fire testing, from which the deign guidance is generally based, is, in general, limited to single elements rather than full structures and cannot capture the full complexities of the structural interactions of a building subject to a real fire. Real fires are more akin to earthquakes from a risk perspective, no two are the same, and a single fire in any given building will affect different elements within the structure differently. Modelling of concrete elements and structures to non-standard fires has shown that long durations of some travelling fires [13] or parametric fires [14] can have significant effects on the fire and post-fire damage and response of concrete structures. However the validity of these models remains in question due to the lack of experimental data, with very few tests conducted in large compartments with travelling fires (e.g. [15]).

To move towards a state where we can assess the fragility of a structure, whether as a driver for design or as a method to assess the damage caused by a fire, data is required. A building's fragility can be assessed empirically from: post-event data (if the intensity of the hazard is quantifiable) or large scale testing (e.g. [16]); analytically, based on simulating the building's performance (e.g. [17]); expert judgment (e.g. [18]), or some combination of these methods.

In many instances the ability to quantify the fire hazard when examining a structure is very difficult, and whilst there has been some large scale full frame response testing of structures exposed to fire, these tests have predominantly concentrated on steel-framed, steel-concrete composite buildings, and only limited research has been performed to quantify the fire fragility of cast-in-place reinforced concrete (RC) structures [19]. In fact, there has only ever been, to the authors knowledge, one large scale multi-storey concrete framed fire test reported in the literature, the Cardington in-situ concrete test [20]. Another notable full scale fire test inside of a concrete building was the Dalmarnock test, performed by the University of Edinburgh, while the focus of these tests was on the fire dynamics some data was collected about the structural response, in particular deflections, strains and through depth temperatures [21]. This paucity of fire testing of concrete framed buildings may be due to the relative simplicity of structural steel materials as compared with concrete, the clear economic advantages of taking a rational approach to structural fire engineering for these types of structures, and the well characterized real life fires that have occurred and large scale experimental programs that have been undertaken in composite steel frame structures (e.g. [22]). This has enabled validation of complex modelling of such structures under multiple credible thermal loading scenarios, and has provided a reasonable amount of data, both analytical and empirical, that can be used in the fire fragility assessment for steel-framed buildings.

Such a rich set of empirical data is not available for reinforced concrete structures exposed to fire, and this prevents detailed and confident validation of models for the full-frame response of RC structures in real fires. Therefore, in this paper, large scale fire testing, analytical modelling, and expert judgment are all used to start to assess the fragility of a concrete column exposed to a fire. This paper presents results from the Tisova Fire Test, a large scale travelling fire test generating experimental data on the thermal and structural response of composite slabs, concrete slabs, and concrete columns. This paper will examine the fire intensity and how it might be quantified; how these quantifications can then be used to model the structural response of the concrete column; and lastly how the modelled response and the quantification of the fire intensity can be used to assess the damage state of the column.

2 FRAGILITY ANALYSES

Fragility analysis thinking has started to appear in the structural fire engineering literature, for example Lange et al. [5] adopted the PEER framework approach in order to analytically assess the annual fire cost of a steel-composite building. In their study, the fire intensity is measured in terms of peak compartment temperature, which has been determined by the use of the Eurocode parametric fire [10], and the response in terms of the deflection of the slab. Repair costs, times and casualties have been associated with thresholds of the deflection mainly based on assumptions. Fragility concepts have predominantly been applied to steel structures (e.g. [23]), however, they have specific relevance for concrete structures since concrete structures have the potential to be repaired following a fire due to low penetration of heat and low residual thermal deformations.

Equation 1 represents the probabilistic risk assessment PEER framework for a building affected by a hazard for a given period of time; for example, fires/year. The risk is defined as consequence × hazard, where the consequence is estimated by three stochastic relationships; intensity measure (*IM*) to response measure (*RM*); RM to damage measure (*DM*); and DM to loss or some other decision variable (*DV*). In other words, given the likelihood of an event occurring in a building, the *IM* forces the building to have a response, *RM*, which leads to a measure of damage, *DM*, and subsequent level of loss, *DV*. The fundamental aim of the reasoning represented by Eq. 1 is to provide quantified annual expected loss metrics for a given structure based on the magnitude and risk of a hazard occurring. A *fragility analysis* is a component of the risk assessment, and consists of two analyses: (1) structural and (2) damage analysis, thus linking the probability of different damage (*DM*) occurring for a given fire intensity (*IM*).

$$gDV = \iiint \overbrace{P[DV \mid DM]}^{\text{Loss analysis}} \underbrace{P[DM \mid EDP]}_{\text{Damage analysis}} \overbrace{P[EDP \mid IM]}^{\text{Structural analysis}} dDMdEDP\underbrace{dgIM}_{\text{Hazard analysis}} \tag{1}$$

These two interrelationships (*IM* to *RM*, and *RM* to *DM*), when coupled, construct a set of fragility curves that correspond to discrete damage states included in a damage scale (see Figure 2). A fragility curve is a continuous fire intensity-to-damage relationship that expresses the probability that a building will suffer damage corresponding to a specific damage state for a given fire intensity measure. Symbolic fragility curves for a hypothetical 4-state damage scale are illustrated in Figure 2.

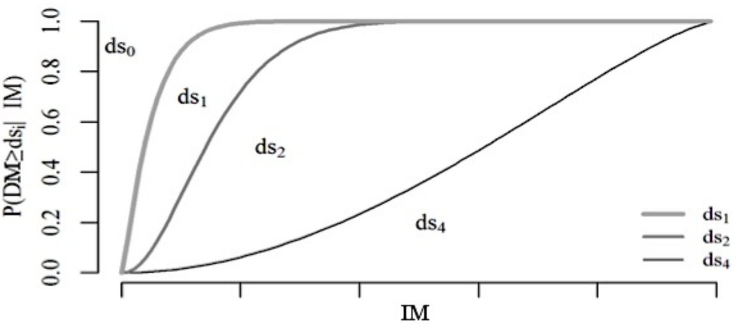

Figure 2: Fragility curve for a hypothetical 4-state damage scale ranging from no damage to structural collapse.

The advantage of Eq. 1 is that it implicitly assumes that that each of the four analyses can be conducted independently, and that the final products of the conditional distributions presented in Eq. 1 can be coupled to estimate the risk to the building over a specified period of time.

The determination of suitable intensity measures is not straightforward since *IM*s also depend on the effect that a hazard has on the structure and the *RM* being assessed (i.e. an *IM* should be chosen which correlates as well as possible with the *RM*). Ideally a large database of experimental and real fire structural response data would inform decisions on which *IM*s and *RM*s are most suitable for use in designing concrete buildings; however, there is a paucity of data, and thus computational analysis and expert opinion must be relied upon (i.e. [24]). Once the *IMs* and *RMs* have been decided, *DM*s can be determined (as has previously been attempted in [4]), along with the costs associated with the *DM*s, through expert opinion. The risk assessment framework of Eq. 1 estimates the risk to buildings affected by all possible fires likely to occur in a given interval and allows designers to design specifically for property protection.

2.1 Fragility curves and damage state scale for reinforced concrete

Essential in the development and application of fragility curves is a quantified damage scale. In June 2014 Ioannou et al. [18] performed an expert elicitation exercise with 13 academic and industrial experts in the design and assessment of reinforced concrete structures to fire. During the exercise the experts helped quantify the Concrete Society's damage scale [4], shown in Table 1, and create fragility curves for concrete slabs and columns. Fragility curves were created, through weighted individual experts' opinions following the Cooke's mathematical method [25] to elicit expert judgements, for four response measures, namely spalling, residual capacity, deflection, and peak rebar temperature.

These four response measures are defined as:

- Spalling - the percentage (%) of the exposed surface area of a given element which has spalled due to heating, such that it could be classed in a given damage state;
- Deflection - the level of deflection, D, measured after cooling, which would be associated with a given damage state, and stated as:

$$D = L/X \tag{2}$$

  where L is the length (span) of the element; X is a parameter which determines the deflection in the mid-span on a slab or the end point of a column (i.e. drift);
- Residual Capacity - the percentage of the residual capacity of the examined element that can be associated with a given damage state, ds_i, assuming the element sustains no other structural damage, i.e., spalling or deformation. Note that the residual capacity was judged as the ratio of total remaining capacity (N_{Res}) to original capacity (N_{Amb}) regarding the axial load capacity for columns and flexural capacity for slabs (i.e. shear capacity is ignored); and
- Peak Rebar Temperatures - the rebar temperature (in ^{o}C) associated with ds_i, again in the absence of spalling.

The four response measures were chosen due to their range of applications in either design or in post-fire assessment. For example, in design, there are very few models to predict spalling of concrete, and deflections of slabs and columns are difficult to predict with accuracy and can be computationally heavy, and are subject to greater modelling uncertainties. Conversely, the peak rebar temperature can be determined relatively simply through heat transfer analysis, and the residual capacity of the column, whilst being a modelling step more, can be determined by applying the calculated temperatures to strength reduction relationships that are well characterised. When post-fire assessments are required, visual and measurable levels of spalling and deflection reduce the uncertainty about these responses, whereas destructive testing of the exposed concrete would be required to ascertain accurately the residual capacity of the element or the peak temperature that the rebar experienced.

Table 1: An example of a visual damage state classification table for reinforced concrete elements (modified from [4])

DS	*Surface Appearance of Concrete*			Description
	Condition of finish	*Colour*[1]	*Crazing*	
ds_0	Unaffected or beyond extent of fire			
ds_1	Some Peeling	Normal	Slight	Damage primarily cosmetic in nature, which does not impact on the design or repair of the structural fabric of RC buildings.
ds_2	Substantial Loss	Pink/ Red	Moderate	A small amount of damage has been experienced by the element to the effect that some small scale remedial action is required to enhance the element's remaining ability to perform its structural functions.
ds_3	Total Loss	Pink/Red Whitish grey	Extensive	The element has experienced a significant, but not catastrophic, amount of damage to the effect that, with significant remedial action, it can be reinstated to perform its structural functions.
ds_4	Destroyed	Whitish grey	Surface Lost	The damage cause by the fire is so extensive that it is no longer viable to repair and reuse the element and replacing the element with a new element is the only option. The building has not suffered a disproportionate collapse.

[1] Table 1 notes the colour of the concrete at different damage states. Not all concrete will change colour in this manner as colour change is due to the concrete's constituent materials.

The expert elicitation exercise performed by Ioannou et al. [18] followed the method created by Cooke [25]. Experts were initially asked to answer 'seed' questions, where the answers were realisable values (i.e. can be found in literature) but were not necessarily known precisely by the experts. The experts were asked to judge these seed values within credible confidence bounds (i.e. 5%ile, mean, and 95%ile). From the seed questions (answered individually and without reference to other experts) the relative ability of each expert to quantify these uncertain values, accurately and informatively, allows a calibration (weighting) of each experts' ability to make judgments.

After the seed questions were answered the experts were asked the experts to judge the relationship of the response to fire intensity (i.e. RM given IM) for three distribution-defining quantiles (5%ile, mean, 95%ile) so that uncertainties around the response given a generic measure of the intensity can be quantified.

In this elicitation the intensity used was the equivalent time of the standard ISO-834 fire, chosen due to its familiarity within both academia and consultancy (as shown in Figure 3). The time equivalency is based on Ingberg's principle [26] that equates the area under the time-temperature curve above 150°C of the standard fire curve (Area A) with the actual fire curve (Area B)

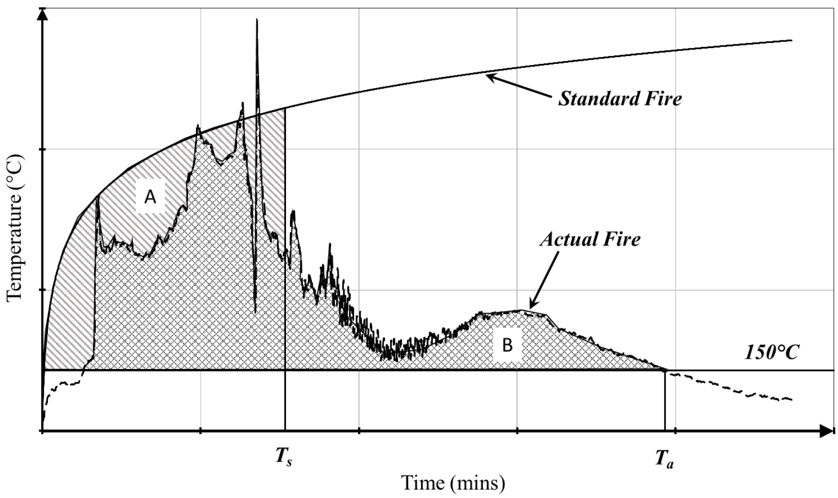

Figure 3: Schematic showing Ingberg's [26] equivalent temperature-time fire curve concept.

Similarly, the experts we asked to judge the relationship of the response given that the element was in a specified damage state (i.e. RM given DM), again for three distribution-defining quantiles (5%ile, mean, 95%ile). The results of the full expert elicitation can be found in Ioannou et al. [18]. From the RM given DM relationship judgments found in the expert elicitation exercise a quantified damage scale for slabs and columns was created as shown in Table 2, which shows the weighted experts mean judgment of the response for that damage state, as well as the upper and lower percentiles to bound the uncertainty. For instance, if a slab had 66% of its residual capacity left, then the experts would expect it to be in damage state 3, however if the slab had as little as 41% or as much as 87% residual capacity, it could still be in damage state 3 but this is judged to be unlikely. Similarly, if the column rebar temperature achieved 190°C, the experts would expect it to be in damage state 2, however there would be an unlikely, but possible, situation where the column could be in damage state 3 (5%ile ds_3 temperature is 170°C).

Table 2: Quantified damage states for reinforced concrete slabs and columns

C	Element	Spalling (% surface area)			Dimensionless parameter X (X=L/D eq. (2))			Residual Capacity (% - N_{Res}/N_{Amb})			Peak Rebar Temperature (°C)		
		5%	95%	mean	5%	95%	mean	5%	95%	mean	5%	95%	mean
ds_0	-												
ds_1	Slab	0.38	13.06	4.75	722.13	24068.88	7357.69	90.16	99.92	97	15.28	157.91	63.2
	Col.	0.24	13.11	4.48	134.05	25956.29	6716.82	91.54	99.91	97	15.93	147.68	60.99
ds_2	Slab	3.42	30.91	14.62	121.74	9109.59	2489.4	75.26	96.62	88	77.82	391.55	196.93
	Col.	2.83	32.62	14.68	84.95	934.54	367.5	82.67	97.26	91	77.17	348.3	182.08
ds_3	Slab	13.64	63.55	36.87	31.15	1650.29	469.61	40.71	87.55	66	190.21	730.63	405.32
	Col.	12.02	61.82	34.88	63.07	222.46	127.47	35.08	95.33	70	169.87	615.82	349.2

ds_4	Slab	36.38	92.79	68.07	7.07	221.93	68.57	4.87	73.77	35	434.97	1037.84	695.77
	Col.	31.27	91.9	64.78	13.6	97.46	43.55	4.12	83.42	39	335.76	986.07	607.09

Having determined the shapes of the fire intensity-to-response and response-to-damage relationships, the fragility curves were constructed by numerically coupling these two relationships, using a method proposed by Porter and Kiremidjian [27] which employs Monte Carlo analysis. A full description of the Monte Carlo analysis used to create the fragility curves is presented in Ioannou et al. [18]. Essentially, for a given intensity measure a random level of cumulative distribution (between 0,1) is chosen. This corresponds to a certain level of structural response estimated from the intensity to response (IM to RM) relationships. This level of structural response could potentially lead to one of five damage states, and the probability that each damage state is reached or exceeded is estimated from the response to damage relationships (RM to DM). Then another random cumulative distribution (between 0,1) value is generated and this value corresponds the structural response value to a specific damage state. This process was then done 10,000 times to create the fragility curves relating the IM to DM.

The fragility curves created, linking the intensity of a fire (in this case the equivalent time of the standard ISO-834 fire) to the probability of being within a certain damage state, can be seen in Figure 4 for each of the four response measures explored. For instance, for a fire intensity of the equivalent of 60 minutes of the standard fire you have, for spalling of a column, a 99% chance of being in at least damage state 1, a 96% chance of being in at least damage state 2, a 78% chance of being in at least damage state 3, and a 37% chance of being in at least damage state 4.

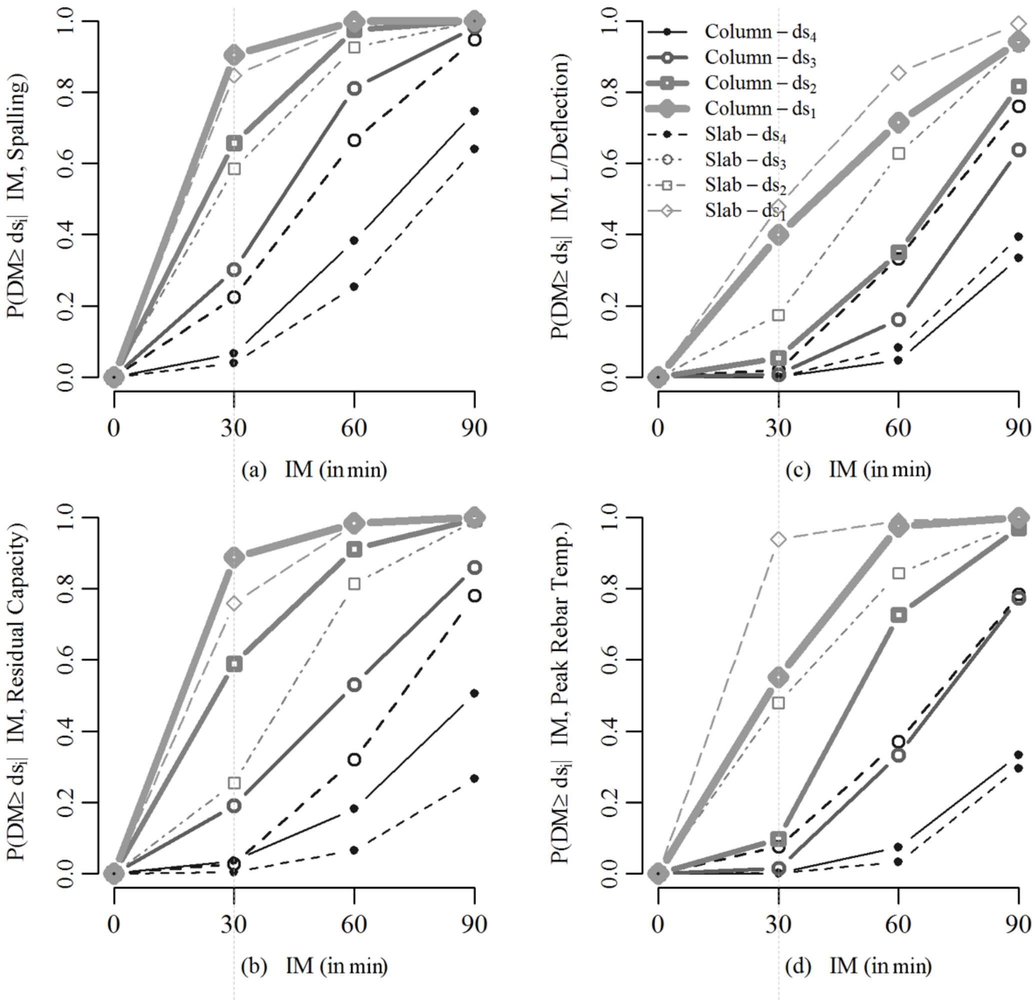

Figure 4: Fragility curves corresponding to three damage states for (a) spalling, (b) deflection, (c) residual capacity and (d) pear rebar temperature constructed for slabs and columns.

Using the quantified damage scale (Table 2) and the fragility curves (Figure 4), an analysis of a column exposed to a travelling fire will now be presented.

3 TISOVA FIRE TEST

The Tisova Fire Test was carried out in January of 2015 by a team lead by SP Technical Research Institute of Sweden and the University of Edinburgh. The fire test was conducted inside of a real building, Figure 5, which was scheduled for demolition. The building was an internal reinforced concrete frame and slab construction and thick load-bearing masonry walls around the perimeter constructed in 1958. In 1980 the buildings use was changed and additional floors were added using composite slab construction tied in to the original frame.

The test compartment shown in Figure 6 was on the ground floor and the fire compartment had a total area of approximately 230m^2 and was 4.4 m high from floor to slab soffit. The layout was generally open, with a series of large rooms enclosing one side as well as one corner. There was also a central lift shaft. Four columns were fully within the fire compartment. The smallest 30 x 30 cm column (C1) indicated in Figure 6 was chosen to be examined due to its slenderness and was therefore most likely to experience higher core temperatures and damage during the fire test.

Ventilation was available by means of four windows on the south facing wall, two on the east facing wall, and one on the north facing wall. All windows were 2,4 m in height. Those on the south facing wall were 2,4 m wide. The window on the North wall was 3,6 m wide. The windows in the East wall were 2,4 m wide.

Figure 5: Left – Southwest corner of test building, and Right – fire compartment

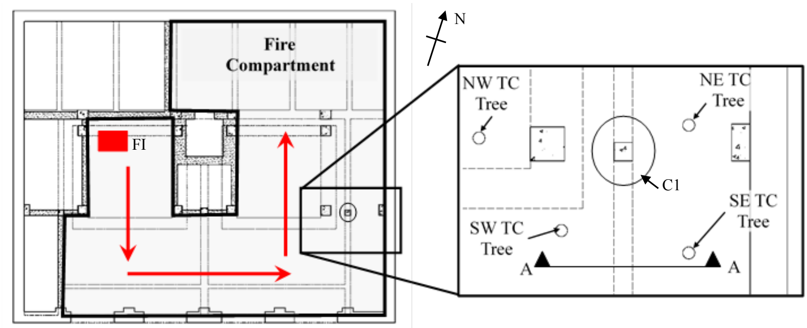

Figure 6: Fire compartment showing fire ignition point (*FI*) and path of travel (arrows), and column C1 and associated TC tree locations

The size and layout in particular of the compartment meant that it was ideal for a fire test which could later allow a comparison with the travelling fires methodology developed by Stern-Gottfried & Rein [28] and improved upon by Rackauskaite in 2015 [29]. Travelling fires are an alternative to the "well-mixed reactor" assumption which is typically made for structural fire design when relying on, e.g. the standard temperature-time curve or a parametric temperature time curve, which results in a uniform temperature throughout a compartment. Observations of the behaviour of fires in real buildings such as the World Trade centre towers 1, 2 and 7 (2001) [30,31]; the Windsor tower in Madrid (2006) [32]; and the Faculty of Architecture building fire at TU Delft (2008) [33] indicate that fires move around floor plates, with an area burning which is dependent on the flame spread rate and the burning rate. Gales also identified travelling fire behaviour in a review of the St Lawrence Burns fire tests carried out in Canada in (1958) [34]. In summary, the travelling fires methodologies divide a large compartment into two distinct regions, a near field with localised burning and a far field with pre heating as a result of a developing hot gas layer and then a continued exposure to the hot gas layer after the travelling near field has passed.

Although only 230 m^2 in area, the test area was significantly larger than the majority of floor areas in fire tests reported in the literature, with the notable exceptions of: the 5th Cardington test (378 m^2) [22]; Car Park Fire Tests conducted as part of an RFCS project in 2002 (512m^2) [35]; and the CESARE fire test conducted by Victoria University in Melbourne, Australia, (320 m^2) [36]. The layout of the compartment was also conducive to having a fire which would spread from the point of ignition, depending on the fire spread rate and the burning rate, and follow the fuel bed along a path which encircled the core of the building. The fuel was laid out as a uniform single fuel bed across the whole floor, apart from a 0.5 – 1 m path around the perimeter of the floor area. Fuel covered approximately 170 m^2 of the floor area as shown in Figure 6. The approximate fuel load made of spruce timber was 40kg/m^2 or 680MJ/m^2. The fire was well ventilated to ensure that fire was fuel load controlled and not controlled by ventilation, and the fire was ignited at location *FI* in Figure 6 using organic fuel soaked in lighter fuel within the crib.

Fire temperatures within the compartment were recorded using 56 thermocouple (TC) trees incorporating Type-K Inconel sheathed thermocouples hung from the ceiling at approximately 2.5m spacing's. Figure 6 shows the four thermocouple trees within a 2.5m radius of the column C1, named NE, NW, SE, and SW TC trees, respectively. Each thermocouple tree had 6 thermocouples at heights below the soffit of the slab of: 5cm, 65cm, 140cm, 205cm, 260cm, and 370cm, respectively. The top of the fuel bed was approximately 40cm off the floor. The SW and SE TC trees are shown in Figure 7: Section A-A.

Column C1 was instrumented with a total of 12 thermocouples, 6 thermocouples positioned 1.5m above the floor and 6 thermocouples 3m above the floor, unfortunately the thermocouples 1.5m above the floor suffered from a failure early on in the test and all data was corrupted and will not be discussed any further in this paper. Figure 7: Section B-B shows the locations of the thermocouples at the 3m height of the column. Figure 7 shows four TCs which were placed 6 cm from each of the four faces, and two TCs which were placed 10 cm from the North and West faces. Holes were drilled at an angle of 45° from above to mid-depth of the columns and TCs were then temporarily held in position and re-cast into the column using quick setting mortar. A plate thermometer (PT) was placed 10 cm from each of the North (N), East (E), South (S), and West (W) column faces with their centres at the same height from the floor as the thermocouple ends as an indication of the fire exposure to the column at the 3m height.

4 RESULTS

The fire was successfully ignited as planned however it soon became evident that fire spread rate was very slow with the flame length along the path (shown in Figure 2) of approximately 1 m with a flame height between 1.5 – 2 m. The resulting temperatures in the compartment, especially near the ceiling, were not high enough for a structurally challenging fire, i.e. well below 100^{o}C. This was due to the overventilation of the compartment provided by the opening of all of the windows. To encourage fire growth during the test the ventilation was reduced and a 10 litre mixture of gasoline and diesel at a ratio of 1:1 was poured over the fuel bed along the southern perimeter 2.5 hrs into the test. This resulted in a more severe fire covering cribs in the west and south ends of the building. However, as the fire started to move north (Figure 2), the intensity of the fire reduced and the fire spread further into the compartment slowed significantly. The reason for the poor severity of the fire was mainly due to the moisture content of the wood, which when controlled specimens were tested after the fire, showed a moisture content between 18-22% rather than 11%. Higher moisture contents results in more energy being absorbed in the evaporation of water rather than into the fire environment, and reduces the rate of flame spread [37]

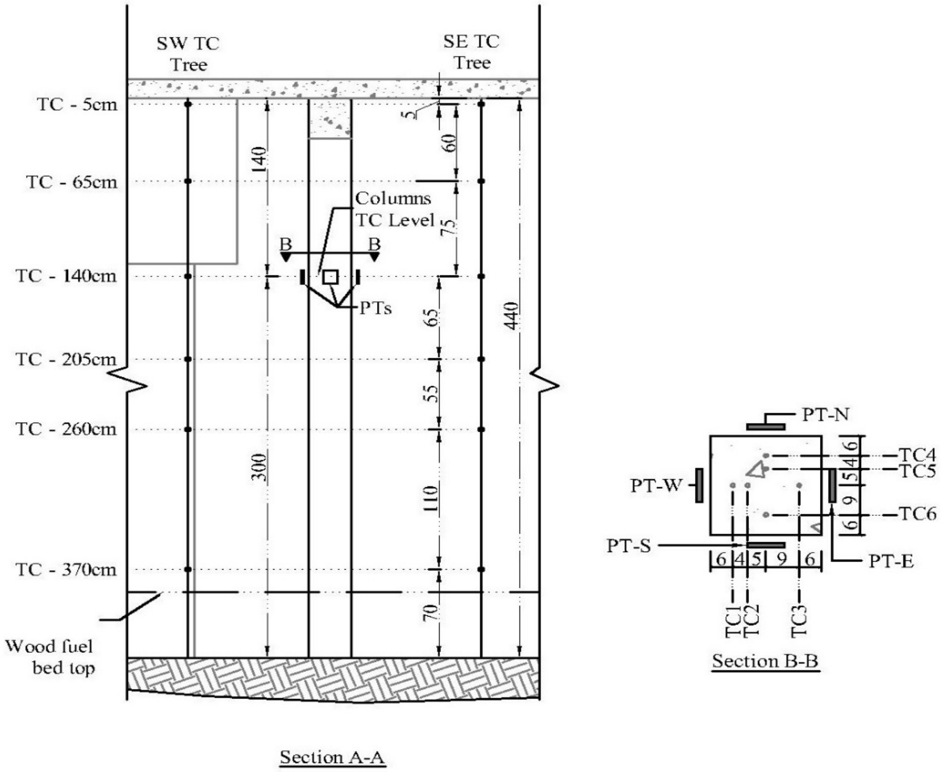

Figure 7: Section A-A: TC tree thermocouple layout, and column TC and PT height, and Section B-B: Column cross-section showing TC and PT placement

4.1 Thermocouple temperatures in region of column

Figure 8 a) shows the recorded temperatures during the fire test at different depths below the soffit of the slab. The slow fire spread rate discussed earlier results in a period of preheating of the thermocouples around the column. The fire stays within the region of ignition for the first 2:30 hrs, and the thermocouples around the column are exposed to only far field heating, especially at the upper levels. The figures show a significant and rapid increase in temperatures recorded by all thermocouples adjacent to the column after 2:30 hrs due to the addition of the gasoline / diesel mix to the fire compartment to encourage the growth of the fire.

When the diesel / gasoline mix is added the fire moves rapidly across the area adjacent to the south facing windows. This could be seen as equivalent to the near field fire exposure, and is characteristic of a faster fire spread and burning rate. The ignition of the diesel / gasoline mix is evidenced by the 'spike' which is seen in Figure 7 a). It can also be seen from Figure 8 a) that the temperatures nearer the ceiling (5cm, 65cm, and 140cm) are fairly consistent across all four TC trees (NW, NE, SW, and SE). Maximum average temperatures experienced in the top 140cm of the fire compartment were in the region of 400-450^{o}C. In contrast the temperatures further away from the ceiling were more varied but in general hotter than those near the ceiling, with average temperatures peaking at 500^{o}C, 635^{o}C, and 510^{o}C, at 205cm, 260cm, and 370cm from the ceiling, respectively. This is clearly shown in Figure 8 b) which shows the variation in temperature over the height of the compartment at 30 minute intervals, with the maximum temperatures, after the gasoline was added at 2:30 hrs, consistently observed within the lower half of the compartment for over two hours. This higher temperature lower down the column is a result of what is effectively a localised fire exposure in the well-ventilated compartment.

As the fire consumed the majority of fuel in the region adjacent to the south facing windows, it also moved into the space to the north- east of the core, and again the thermocouples closer to the ceiling are exposed to higher temperatures, characteristic of the far field exposure once the near field has passed.

4.2 Plate thermometer data

The thermal boundary for the column at 3m above the floor was measured using four plate thermometers (PT) around the perimeter of the column (Figure 7: Section B-B). Figure 9 a) shows the recorded PT temperatures for the individual PTs and compares the average temperatures from the PTs to the average TC-140cm temperature data, showing a very good correlation between the two averages. Any future modelling of the heat transfer to the column can be confident of the thermal boundary present in the tests.

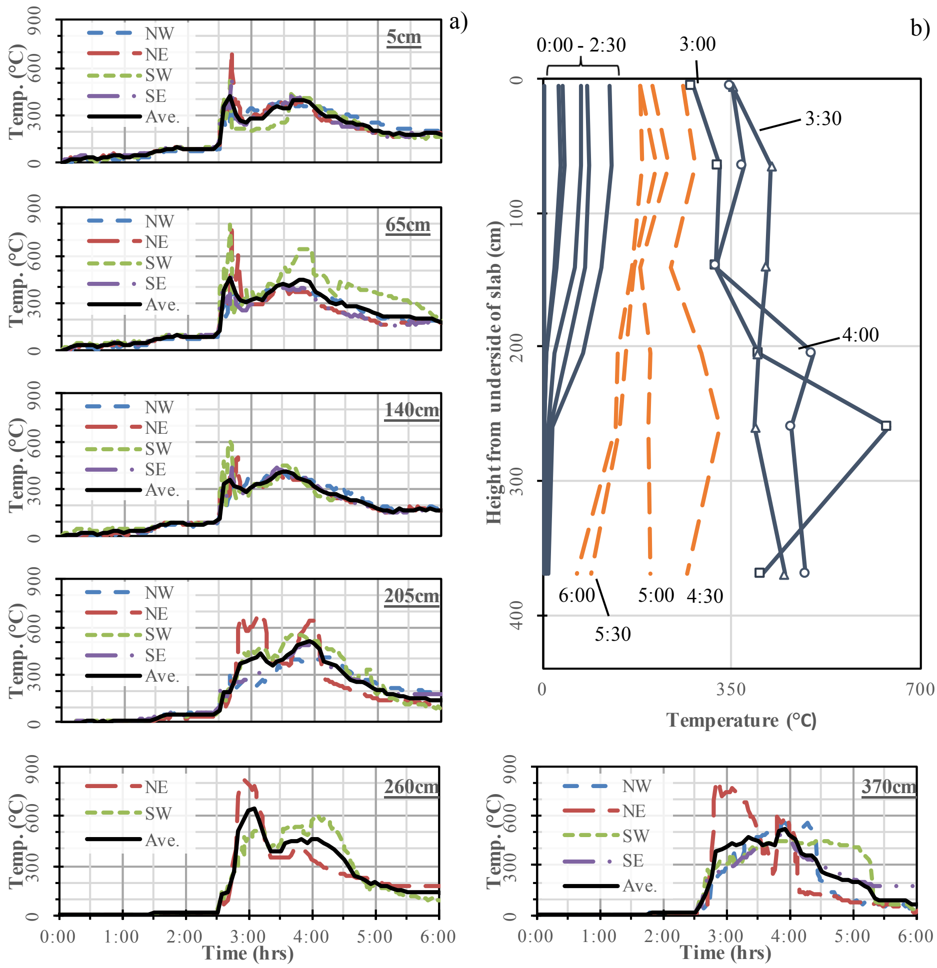

Figure 8: a) Time-temperature curves at each of the 6 TC heights below the soffit of 5cm, 65cm, 140cm, 205cm, 260cm, and 370cm; and b) variation in temperature over the height of the compartment at 30 minute intervals

4.3 Column temperature data

As previously stated, unfortunately temperatures at 1.5m above the floor failed to be recorded, so comparisons of the heat transfer to the column from the more severe temperatures recorded within the lower half of the compartment to the cooler upper half cannot be made. However, Figure 9 b) shows the data recorded at 3m above the floor (1.4m below the ceiling), and shows an increase in structural temperatures at around 2:40 which increase relatively linearly until 4:30 at approximately $1^{o}C/min$. The very slow heating rate causes very similar temperatures to be observed within the cross-section.

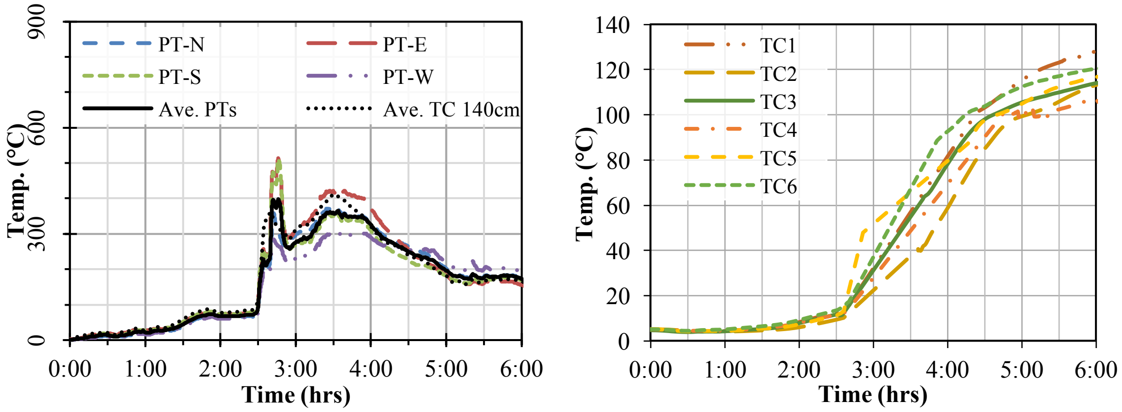

Figure 9: a) Comparison of PT and TC tree recorded temperatures at 140cm below ceiling soffit; and b) Recorded temperatures within concrete column C1

4.4 Material Testing

There were two types of concrete present within the building; one as used for the original reinforced concrete construction; and the other as used for the composite slabs added in 1980. Cores, 100 mm in diameter, were taken from the elements taken in the building before the fire and were tested to ascertain their material properties. Cores were also taken after the fire to assess the mechanical damage to the concrete due to the heating – however due to a mis-communication a post-fire core of the concrete column examined here was unfortunately not taken.

4.4.1 Thermal Conductivity

The thermal conductivity of the concrete in the building was determined based on TPS measurements [38] of 100 mm diameter cores of the elements taken from the building. The TPS measurements were made up to 300 °C, and then extrapolated to 1000 °C. The thermal conductivity of the reinforced concrete column was approximately half way between the upper and lower limits. The specific relationship between conductivity and temperature for the reinforced concrete column is given in equation (2).

$$\lambda = \left(1.70 - 0.195\left(\frac{T}{100}\right) + 0.0085\left(\frac{T}{100}\right)^2\right) \Big/ 1000 \tag{2}$$

4.4.2 Specific heat

Specific heat of the concrete was measured using the TPS heat capacity module. This was found to be the same as the specific heat of dry concrete given in the Eurocode [9]. The moisture content of the concretes, determined through drying of a specimen at 105 °C for 24 hours was determined to be 1.15 % by weight.

4.4.3 Mechanical properties

The compressive strength of the concrete in the building was determined by cylinder tests based on additional cores taken from the building. The concrete used in the reinforced concrete column had a compressive strength of 32MPa. These measurements are based on only one series of tests and are only indicative of the strength of the concrete in the building.

5 MODELLING AND ASSSESSMENT OF DAMAGE

In designing a building or assessing a fire-damaged structure, unlike in the tests presented above, the exact time-temperature history of the fire is very unlikely to be known. For post fire assessments when the temperature-time history is not known, then a visual assessment of the element(s) can be used to provide some information about the condition of the specimen, for example colour changes can give an indication of the maximum temperatures observed. Using a general measure of intensity one can assess different fire scenarios, then these fire scenarios can be applied to the structure or element to quantify its response, from which, with a quantified damage state scale, it is possible to understand the damage to a structure or element.

5.1 Visual and mechanical post-fire assessment

Using the visual descriptors of damage presented in Table 1 an assessment of the damage to the column was made. A visual inspection of the column showed no obvious signs of damage (i.e. no spalling & no out of straightness) apart from aesthetic smoke damage, this would mean that the column could be in either damage states, ds0 or ds1.

5.2 Modelling assessment of the damage

Three heights along the column were chosen to be investigated in this analysis; 1) 65cm below the soffit due to the time-temperature curve having the greatest total area under the fire curve at this height; 2) 140cm below the soffit due to the additional plate thermometer temperatures and the internal concrete temperatures that can be used to benchmark thermal modelling of the concrete column; and 3) 260cm below the soffit due to the highest recorded temperatures observed at this height.

5.2.1 Assessment of the intensity

Using the fragility curves presented in Figure 4 and a measure of the intensity of the fire, it is possible to estimate the damage state that the concrete column is in. To generate a measure of the intensity the recorded time-temperature histories at the three depths below the soffit are converted in to equivalent areas under the standard fire curve based on three levels of equivalency being assessed; the total area under the curves; the total area above 150°C [26]; and the total area under the curve above 400°C [14]. The equivalent area concept is shown in Figure 3, and the values of the equivalent time under the ISO-834 fire [39] are presented in Table 3. These equivalent fires are applied as the measure of intensity within the fragility curves (Figure 4) from which the likelihood of the column being in one of the damage states can be assessed by reading the probability associated with a given damage state at that intensity off the graph. For example, for spalling damage shown in Figure 4 a), the probability of the column being in Damage State 4 at an intensity of 60 minutes is around 40 %; the probability of the column being in Damage State 3 is around 80 %; the probability of it being in Damage State 2 is ca.97 % and the probability of it being in Damage State 1 is almost 100 %. Table 3 shows for comparison the highest damage state, for each of the measures of damage, at the different intensities, for which the probability of the column being in that damage state is greater than 50 %.

Table 3: Equivalent ISO exposures and expected damage states from fragility curves

Depth below soffit (cm)	Recorded area under time-temperature the curve (Temp.mins)			Equivalent time under ISO-834 (mins)			Expected Damage State P(DM>ds*i*$\mid$IM)											
							Spalling			L/Deflection			Residual Capacity			Peak Rebar Temperature		
	total	>150°C	>400°C	total	>150°C	>400°C	total	>150°C	>400°C	total	>150°C	>400°C	total	>150°C	>400°C	total	>150°C	>400°C
65	82785	35374	1772	95	46	4	ds4	ds3	ds0	ds3	ds1	ds0	ds4	ds3	ds0	ds3	ds2	ds0
140	64824	22849	146	77	32	0	ds4	ds2	ds0	ds3	ds1	ds0	ds3	ds2	ds0	ds3	ds2	ds0
260	76529	39418	9083	89	51	15	ds4	ds3	ds0	ds3	ds1	ds0	ds4	ds2	ds0	ds3	ds2	ds0

As can be seen from Table 3 there is great variance between the intensity measures depending on the method used to assess it, and this then translates into the expected damage state assessment. For instance, the residual capacity of the column using the total area under the curve equivalency expects the column to be in damage state 4, and therefore in need of replacement rather than repair. The same column using the area under the curve above 400°C expects the column to be in damage state 0 and therefore unaffected by the fire. This shows the importance of selecting the appropriate measure of intensity when conducting fragility analyses.

5.2.2 Assessment of the response

The above showed one method to assess the damage to an element if the intensity of the fire is known through the use of fragility curves, and if desired the quantified damage could be estimated through the use of the quantified damage state scale presented in Table 2. Another method to assess the damage from the known fire is to determine the response of the concrete from the intensity and then assess the damage for a particular response measure. In this paper the thermal profile of the concrete will be modelled through ABAQUS, and then an estimation of the loss in concrete strength due to the maximum temperatures the cross-section experiences.

Initially the concrete cross-section at 140cm below the slab soffit was modelled using ABAQUS, employing thermal boundary properties (ε_{tot}=0.7, α_c=25 W/m^{2}K) including the recorded temperature history, and concrete thermal properties mentioned previously. As can be seen in Figure 10, the modelled temperatures are in general slightly greater compared to the averaged recorded temperatures. The average error over the 6 hours is -2.3^{o}C and +8.6^{o}C, with maximum absolute errors of 17^{o}C and 25^{o}C, for TC's 2 & 5 and TC's 1, 3, 4, & 6 respectively. These relatively small errors are likely due to inaccuracies of retrofit placement of the thermocouples within the column and modelling a 3D environment in 2D. However, these errors are within expected levels experimental and modelling errors.

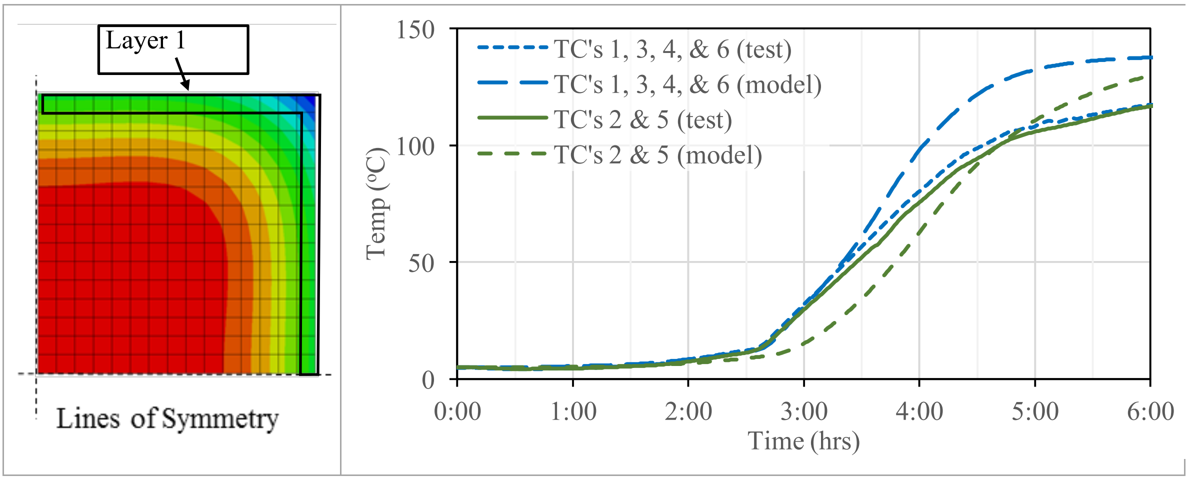

Figure 10: a) quarter cross-section of column at 6hrs of heating; and b) comparison of modelled and recorded average temperatures within cross-section.

Using the benchmarked thermal model, two subsequent thermal analyses assessed the thermal profile of the cross-section at the 65cm and 260cm depths below the soffit. The cross-section was also modelled to the three levels of equivalent times (see Table 3) under the ISO-834 time-temperature curve. The thermal response of the cross-section is compared in Figure 11 which shows the averaged maximum temperature at the centroid of the cells for each layer of cells at a perpendicular distance from the centroid (schematic shown for layer 1 in Figure 10 a)), determined using recorded thermocouple temperatures (Real) or equivalent durations of the ISO-834 fire using either the total area under the curve, area under the curve above 150^{o}C, or area under the curve above 400^{o}C. Figure 11 clearly shows that any of the equivalent area methods do not accurately predict the thermal gradients experienced within the concrete column when it is exposed to a travelling fire.

From the thermal models, two assessments of the damage can be made; 1) the relative reduction in concrete strength and thus the residual capacity of the column, and 2) the peak rebar temperature. For the assessment of the residual capacity of the column a few assumptions have been made. Firstly, that the concrete is made of siliceous concrete, secondly that the steel rebar regains all of its strength after heating whilst the concrete regains none, and lastly that the reduction of concrete capacity can be determined by taking the weighted average of temperature dependent reduction factors for each layer of cells at a perpendicular distance from the centroid. It should be noted that some experimental campaigns and literature [40] show that the strength of concrete can further reduce after cooling but the degree of reduction is not clear. The Eurocodes [41] suggest a 10% additional decrease during cooling however it has been shown that this could be anywhere between 0-25% [40] and therefore we have not included it in this analysis . For the assessment of peak rebar temperature, the assumption is that the steel rebar has a clear cover depth of 30mm due to lack of other pertinent data. The peak rebar temperatures and relative loss of capacity of the concrete and steel strengths during heating can be seen in Table 4.

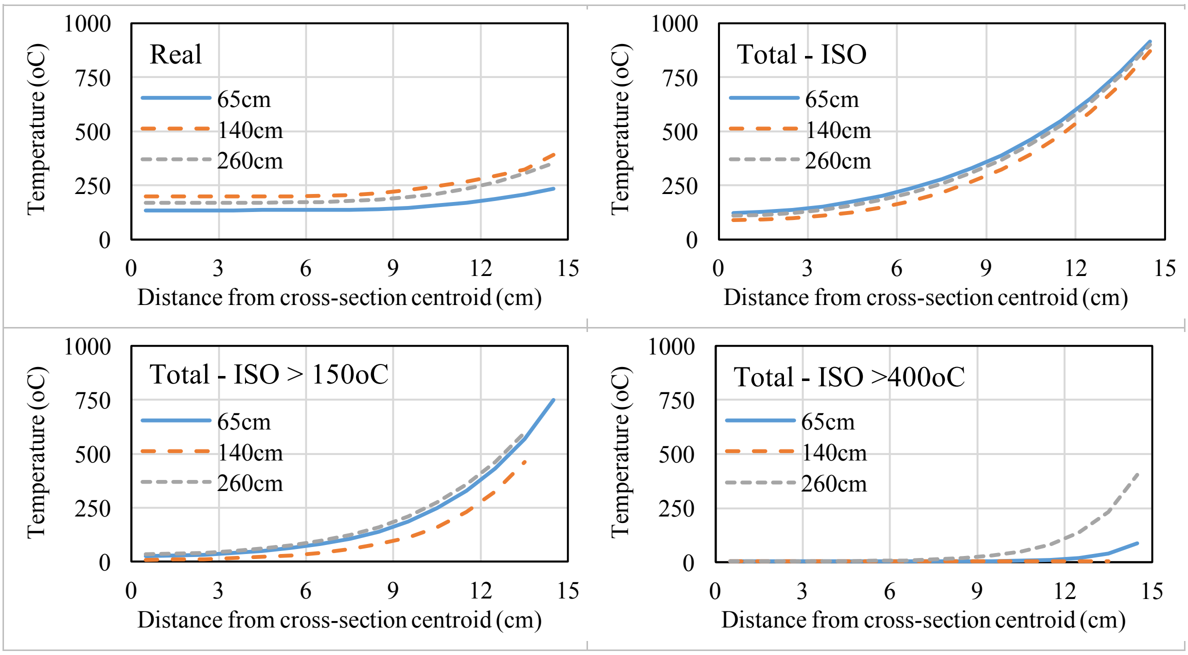

Figure 11: Maximum temperature profiles under real travelling fire, and equivalent times under the ISO-834 fire curve

Table 4: Averaged concrete and steel rebar strength reduction factors and peak rebar temperatures due to real and equivalent fire exposures

Depth below soffit (cm)	Equivalent time under ISO-834 (mins)			Average concrete cross-section reduction factors $f_{c\theta}/f_{ck}$				Steel rebar reduction factors $f_{s,\theta}/f_{yk}$				Peak rebar temperature ℃			
					ISO equivalent area				ISO equivalent area				ISO equivalent area		
	Total	>150°C	>400°C	Real	total	>150°C	>400°C	Real	total	>150°C	>400°C	Real	total	>150°C	>400°C
65	95	46	4	0.94	0.57	0.74	1	1	0.63	1	1	210	549	328	10
140	77	32	0	0.97	0.63	0.82	1	1	0.82	1	1	172	482	230	5
260	89	51	15	0.9	0.59	0.72	0.96	1	0.69	1	1	283	528	357	82

Table 5: Assessment of the damage state of the column at each depth below the soffit based on reduction factors and peak rebar temperatures presented in Table 4

Depth below soffit (cm)	Equivalent time under ISO-834 (mins)			Damage state							
				Residual Capacity				Peak Rebar Temperature			
					ISO equivalent area				ISO equivalent area		
	Total	>150°C	>400°C	Real	total	>150°C	>400°C	Real	total	>150°C	>400°C

65	95	46	4	ds2/*ds1*	ds3/*ds4*	ds3	ds0	ds2/*ds3*	ds4/*ds3*	ds3	ds0
140	77	32	0	ds1	ds3/*ds4*	ds3	ds0	ds2/*ds3*	ds3/*ds4*	ds3/*ds2*	ds0
260	89	51	15	ds2/*ds3*	ds3/*ds4*	ds3	ds1	ds2/*ds3*	ds4/*ds3*	ds3	ds1

Table 4 shows that the column loses 3%-10% of its capacity in the concrete under the real traveling fire scenario, with the maximum losses of capacity occurring at 260cm below the soffit. The loss in strength when the section is modelled using the total equivalent area under the fire curves is between 37% - 43%, whereas for equivalent areas above 150^{o}C, losses in the concrete are between 18% - 28%. It is only when the equivalent areas above 400^{o}C is used that we get close to what is modelled, in terms of strength loss for both the steel and the concrete, from the real travelling fire scenario. This shows the significance of both the area and maximum temperatures of the time-temperature history of the travelling fire when trying to create an equivalent time of exposure to the ISO-834 standard fire.

The concrete strength reduction factors (used as a proxy for residual capacity of the column based on the assumption that the steel will regain its strength) and peak rebar temperature can be used to assess the damage state of the concrete column at the different depths below the soffit with careful comparison to the quantified damage scale presented in Table 2. The damage state for each of the four fire intensity measures for the two examined response measures are presented in Table 5. As there is some uncertainty within the quantified damage scale there are occasions where the calculated response could fall into one of several potential damage states, which has been signified in Table 5 with the use of plain text for the most likely damage state (i.e. ds0) and italicised text for possible but less likely (i.e. /*ds1*). It can be seen from Table 5 that the predicted damage states using the equivalent areas of fire duration compare poorly with the damage states determined using the actual time temperature curve, however, there is consistency between the two response measures for the same level of intensity (i.e. *>150^{o}C,* the residual capacity and peak rebar temperatures would put the column in damage state 3.)

5.3 Comparison of damage analyses

The damage states have been assessed using three different methods, 1) a visual assessment measuring the spalling and deflection of the concrete column; 2) from a heat transfer analysis using the real time-temperature history, and equivalent time of exposure to the standard fire curve to assess the residual capacity and the peak rebar temperatures of the concrete column; and 3) using the equivalent times with fragility curves developed through expert judgments to assess the damage with respect to all four response measures. The visual assessment of the columns would see the column in damage state 0, i.e. no damage, while the real time-temperature analysis shows that the column is most likely to be in damage state 2, but with the possibility of being in damage state 1 or damage state 3, and thus in need of repair. When the time equivalence method was used to calculate the residual capacity and peak rebar temperatures, all three of the ISO equivalent area intensity measures compare poorly with the real time-temperature analysis, with both the *total* and *>150^{o}C* placing the column in higher damage states, and the *>400^{o}C* placing it in a lower damage state, than the real time-temperature analysis. This could be because the equivalent area method does not properly produce comparative fire intensities between those used in modelling and the observed time-temperature history of the compartment.

When the equivalent times of fire exposure was used in conjunction with the fragility curves developed from an expert elicitation we find that the damage states determined from the *total* area under the curve are, reassuringly, similar to those found using heat transfer analysis and the quantified damage state table, for the residual capacity. However, when considering the peak rebar temperatures, the heat transfer analysis expects greater damage to occur to the column than the experts do in the elicitation exercise. A similar trend is also seen with the areas *>150^{o}C* and the *>400^{o}C*, with greater damage being determined through heat transfer analyses than from the expert elicitation. More experimental and computational analyses are required to determine and refine the differing methods to assess the fire damage to concrete columns under real fire conditions.

6 CONCLUSIONS

This paper has presented a quantified damage scale and accompanying fragility curves for reinforced concrete columns and slabs. Using these fragility curves and damage scales a damage analysis was presented considering a column exposed to a real travelling fire from the large scale Tisova Fire Test conducted in the Czech Republic in January 2015. From these analyses we can conclude that:

1. A visual assessment of the column would indicate that there would be little to no damage, however, through the use of computational analysis and the application of quantified damage scales generated from expert judgements, the column would likely be in damage state 2 and would thus need some repairing.
2. The well-known equivalent area method for fire intensity does not fully account for the temperature history of long duration travelling fires and therefore, when adopted in these analyses, poorly predicts the thermal profiles within the concrete, or the associated response measures of the column and thus poorly predicts the damage.
3. The use of the equivalent area intensity measures with the fragility curves generated through expert judgement does show a good correlation to the modelling analysis when using the same equivalent area intensity measures, but again poorly predicts the damage when the real time-temperature history is used in the modelling.
4. The calculated strength loss of the concrete column varied between 3-10%, with the greatest occurring under a combination of high temperatures and large area under the fire curve, rather than just due to the latter.

Further research is required to; a) appropriately define the intensity of fires, particularly for concrete elements and structures exposed to long duration fires, b) refine the fragility curves for reinforced concrete elements and structures, and c) to refine the quantified damage scale for concrete elements and structures.

7 ACKNOWLEDGEMENTS

The authors would like to express their most sincere thanks to; all of the firefighters of the fire and rescue service in Carlsbad for their enthusiastic support, the BRE Centre for Fire Safety Engineering; students from Imperial College London, Luleå Technical University, the University of Edinburgh and Technical University Ostrava; and thanks to Majaczech, CSTB and CERIB. The work reported has been carried out within projects supported financially by grants from the Swedish Fire Research Board (Brandforsk), and from the Engineering and Physical Sciences Research Council in the UK (EPSRC – EP/K022369/1).

8 REFERENCES

[1] Wang YC, Burgess I, Wald F, Gillie M. Performance-Based Fire Engineering of Structures. CRC Press; 2013.
[2] The Geneva Assocation. Costs of Direct Fire Losses 2014.
[3] CEN. BS EN 1992-1-2:2004: Eurocode 2: Design of concrete stuctures; Part 1-2: General rules - Structural fire design. Brussels, Belgium: 2008.
[4] The Concrete Society. Assessment, design and repair of fire-damaged concrete structures - Technical report no. 68. Camberley UK: The Concrete Society; 2008.
[5] Lange D, Devaney S, Usmani A. An application of the PEER performance based earthquake engineering framework to structures in fire. Eng Struct 2014;66:100–15. doi:10.1016/j.engstruct.2014.01.052.
[6] Porter KA. An Overview of PEER's Performance-Based Earthquake Engineering Methodology. ICASP9, July 6-9, vol. 273, San Fransico: 2003.
[7] Kam WY, Pampanin S, Elwood K. Seismic performance of reinforced concrete buildings in the 22 Feburary Christchurch (Lyttelton) eathquake. Bull New Zealan Soc Earthq Eng 2011;44:239–78.
[8] Bisby L, Mostafaei H, Pimienta P. State-of-the-Art on Fire Resistance of Concrete Structures: Structure-Fire Model Validation. Appl Res Assoc 2014:32. doi:10.1017/CBO9781107415324.004.
[9] CEN. BS EN 1992-1-2:2004 - Eurocode 2 : Design of concrete structures — Structural fire design. vol. 3. Brussels, Belgium: 2010.
[10] CEN. BS EN 1991-1-2:2002 Eurocode 1- Actions on structures; Part 1-2: General Actions - Actions on structures exposed to fire. vol. 3. Brussels, Belgium: 2009.
[11] Gales J, Maluk C, Bisby L. Large- scale structural fire testing- How did we get here, Where are we, and where are we going? 15th ICEM, Porto, Portugal: 2012, p. 1–22.
[12] Tang M, Castro E, Pedroni F, Brzozowski A, Ettouney M. Performance-Based Design with

Application to Seismic Hazard. Struct Mag 2008:20–2.
[13] Law A, Stern-Gottfried J, Gillie M, Rein G. The influence of travelling fires on a concrete frame. Eng Struct 2011;33:1635–42. doi:10.1016/j.engstruct.2011.01.034.
[14] Rush D, Bisby L, Ioannou I, Rossetto T. Towards fragility analysis for concrete buildings in fire: residual capacity of concrete columns. 8th SiF, Shanghai: 2014, p. 467–74.
[15] Horová K, Wald F, Bouchair A. Travelling Fire in Full-Scale Experimental Building. Des. Fabr. Econ. Met. Struct., Berlin, Heidelberg: Springer Berlin Heidelberg; 2013, p. 371–6. doi:10.1007/978-3-642-36691-8_56.
[16] Rossetto T, Elnashai A. Derivation of vulnerability functions for European-type RC structures based on observational data. Eng Struct 2003;25:1241–63. doi:10.1016/S0141-0296(03)00060-9.
[17] Rossetto T, Elnashai A. A new analytical procedure for the derivation of displacement-based vulnerability curves for populations of RC structures. Eng Struct 2005;27:397–409. doi:10.1016/j.engstruct.2004.11.002.
[18] Ioannou I, Aspinall W, Rush D, Bisby L, Rossetto T. Expert Judgement -Based Fragility Assessment of Reinforced Concrete Buildings Exposed to Fire. Reliab Eng Syst Saf 2017. doi:10.1016/j.ress.2017.05.011.
[19] Bisby LA. Engineering solutions for structures in fire: Should concrete care? In: Zingoni. A, editor. Res. Appl. Struct. Eng. Mech. Comput., Taylor & Francis; 2013, p. 699–700. doi:doi:10.1201/b15963-351.
[20] Bailey C. Holistic behaviour of concrete buildings in fire. Proc ICE - Struct Build 2002;152:199–212. doi:10.1680/stbu.2002.152.3.199.
[21] Gillie M, Stratford T. Behaviour of the Structure during the Fire. In: Rein G, Abecassis Empis C, Richard C, editors. Dalmarnock Fire Tests Exp. Model., 2007, p. 149–60.
[22] British Steel Plc. The behaviour of multi storey steel framed building in fire. 1999.
[23] Gernay T, Elhami Khorasani N, Garlock M. Fire fragility curves for steel buildings in a community context: A methodology. Eng Struct 2016;113:259–76. doi:10.1016/j.engstruct.2016.01.043.
[24] Moss P, Abu AK, Dhakal R. Intesntiy measures for probabilistic structural fire engineering. In: Galock M, editor. SiF 2016, Princeton: 2016, p. 933–41.
[25] Cooke RM. Experts in Uncertainty: Opinion and Subjective Probability in Science. Oxford Univeristy Press; 1991. doi:10.1016/0040-1625(93)90030-B.
[26] Ingberg SH. Tests of the severity of building fires. NFPA Q 1928;22:43–61.
[27] Porter K, Kiremidjian A, LeGrue J. Assembly-based vulnerability of buildings and its uses in seismic performance evaluation and risk managment decision-making. Earthq Spectra 2001;17:291–312. doi:10.1193/1.1586176.
[28] Stern-Gottfried J, Rein G. Travelling fires for structural design-Part II: Design methodology. Fire Saf. J., vol. 54, 2012, p. 96–112. doi:10.1016/j.firesaf.2012.06.011.
[29] Rackauskaite E, Hamel C, Law A, Rein G. Improved formulation of travelling fires and application to concrete and steel structures. Structures 2015;3:250–60. doi:10.1016/j.istruc.2015.06.001.
[30] NIST. Federal Building and Fire Safety Inverstigation of the World Trade Centre Disaster: Final Report on the Collapse of the World Trade Center Towers. Gaithersburg, MD: 2005.
[31] NIST. Final Report on the Collapse of World Trade Center Building 7, Federal Building and Fire Safety Investigation of the World Trade Center Disaster. Gaithesburg, MD: 2008.
[32] Fletcher IA, Borg A, Hitchen N, Welch S. Performance of concrete in fire: A state of the art, with a case study of the Windsor Tower fire. 4th Int. Work. Struct. Fire, 2006, p. 779–90.
[33] Meacham B, Park H, Engelhardt M, Kirk A, Kodur V, Straalen IJ, et al. Fire and Collapse , Faculty of Architecture Building , Delft University of Technology : Data Collection and Preliminary Analyses. 8th Int. Conf. performance-based cosed Saf. Des. methods, Lund, Sweden: 2010.
[34] Gales J. Travelling Fires and the St. Lawrence Burns Project. Fire Technol 2014;50:1535–43. doi:10.1007/s10694-013-0372-3.
[35] Joyeux D, Kruppa J, Cajot LG, Schleich JB, Van de Leur P, Twilt L. Demonstration of real fire tests in car parks and high buildings. 2002.
[36] Proe DJ. Results and analysis of a large-scale fire test on a multi-bay composite steel-frame floor system. J Struct Fire Eng 2016;7:19–29. doi:10.1108/JSFE-03-2016-002.
[37] Fons WL, Clements HB, George PM. Scale effects on propagation rate of laboratory crib fires. Symp Combust 1963;9:860–6. doi:10.1016/S0082-0784(63)80092-2.
[38] Adl-Zarrabi B, Boström L, Wickström U. Using the TPS method for determining the thermal

properties of concrete and wood at elevated temperature. Fire Mater 2006;30:359–69. doi:10.1002/fam.915.
[39] ISO. ISO 834: Fire resistance tests-elements of building construction. Geneva, Switzerland: 1999.
[40] Li Y-H, Franssen J-M. Test Results and Model for the Residual Compressive Strength of Concrete After a Fire. J Struct Fire Eng 2011;2:29–44. doi:10.1260/2040-2317.2.1.29.
[41] CEN. BS EN 1994-1-2:2005: Eurocode 4 — Design of composite steel and concrete structures — Part 1-2: Genreal rules - Structural fire design. vol. 3. Brussels, Belgium: 2008.